Original Article

Eur J Breast Health
DOI: 10.4274/ejbh.galenos.2025.2025-6-2

ROPN1 Gene Expression as a Prognostic and Predictive Biomarker in Aggressive Breast Cancer: Clinical Implications and Survival Association

Ricardo Cesar Cintra[1], Andrés Galindo Céspedes[2,3,4], Olinda Maria Gamarra[5], Carlos Javier Melgarejo[5], Daniel Rodrigues de Bastos[5]

[1]Center for Translational Research in Oncology, Instituto do Cancer do Estado de São Paulo ICESP, Hospital das Clinicas da Faculdade de Medicina da Universidade de São Paulo FMUSP HC, São Paulo, Brazil
[2]Facultad de Ciencias Biológicas, Universidad Nacional Pedro Ruiz Gallo, Lambayeque, Perú
[3]Hospital Nacional "Almanzor Aguinaga Asenjo", Chiclayo, Perú
[4]Universidad Católica Santo Toribio de Mogrovejo, Chiclayo, Perú
[5]Facultad de Ciencias Médicas, Universidad Privada del Este filial Ciudad del Este, Paraguay

ABSTRACT

Objective: The *ropporin-1* (*ROPN1*) gene, initially linked to sperm motility, is differentially expressed in triple negative breast cancer (TNBC), suggesting a role in tumor progression and therapy resistance. To characterize *ROPN1* expression in breast cancer and evaluate its association with clinicopathological features, survival, and treatment response as a translational biomarker.

Materials and Methods: Data from The Cancer Genome Atlas (1,087 patients), Sweden Cancerome Analysis Network-Breast (3,273 patients), and geodatabases were analyzed. *ROPN1* transcriptional levels were assessed in relation to clinical variables and survival. Chemotherapy agents and epigenetic modulators were tested in cell lines to evaluate *ROPN1* regulation.

Results: Transcriptional overexpression of *ROPN1* was significantly enriched in TNBC/basal-like tumors (p<0.0001) and correlated with reduced overall survival, particularly in basal cases [hazard ratio (HR) = 1.85; 95% confidence interval (CI): 1.02–3.33; p = 0.041]. Patients treated with chemotherapy and exhibiting high *ROPN1* levels had unfavorable prognosis, with an even poorer profile in untreated cohorts (HR = 4.55; 95% CI: 1.33–14.29; p = 0.01). Hypomethylation at cg00101712 (HR = 0.59; p = 0.016) and cg09298623 (HR = 0.49; p = 0.0014) CpG sites were associated with worse survival at 5 years follow-up, underscoring epigenetic regulation of this pathway as a key driver of poor outcomes. Furthermore, *in vitro* treatment with cisplatin, doxorubicin, and paclitaxel resulted in variable responses, with a significant reduction of *ROPN1* in HCC70 and HS578T cell lines, while BT549 and MDA-MB-231 cell lines showed notable increases.

Conclusion: *ROPN1* overexpression in TNBC/basal-like tumors suggests a role as a prognostic biomarker and predictor of post-chemotherapy resistance. Investigation of *ROPN1* expression in breast tumors may lead to alternative strategies targeting pro-metastatic pathways and improve precision treatment for aggressive breast cancer.

Keywords: ROPN1; triple negative breast cancer; basal-like; aggressive breast cancer

Cite this article as: Cintra RC, Céspedes AG, Gamarra OM, Melgarejo CJ, de Bastos DR. *ROPN1* gene expression as a prognostic and predictive biomarker in aggressive breast cancer: clinical implications and survival association. Eur J Breast Health. [Epub Ahead of Print]

Key Points

- The *ropporin-1* gene (*ROPN1)* overexpression is linked to worse overall survival, especially in triple negative or basal-like breast cancer.
- High *ROPN1* levels predict poor prognosis in both chemotherapy-treated and untreated patients.
- *ROPN1* expression inversely correlates with DNA methylation and it is known that hypomethylation is associated with adverse outcomes.
- *In vitro*, cisplatin, doxorubicin, and paclitaxel variably modulated *ROPN1* expression in different cancer cell lines with increased expression levels in some cell lines, suggesting therapy resistance.
- Treatment with 5-aza-2′-deoxycytidine or trichostatin-A led to increased *ROPN1* expression.

Corresponding Author:
Daniel Rodrigues de Bastos MD; danielbastos.adm@gmail.com

Received: 11.06.2025
Accepted: 04.08.2025
Epub: 04.09.2025

Introduction

Breast cancer remains the most commonly diagnosed malignancy in women, comprising 24.5% of cases with over 2.3 million new diagnoses annually, and is the leading cause of female cancer death (685,000 deaths in 2020) (1). The incidence of breast cancer is higher in developed countries, reflecting both lifestyle factors and advanced screening, whereas delayed diagnosis and limited therapy access drive elevated mortality in low- and middle-income regions (2, 3). By 2040, cases are projected to exceed 3 million, with over 1 million deaths (4).

From a molecular perspective, breast cancer is a heterogeneous disease classified into distinct subtypes based on gene expression profiles and biomarker presence. The main molecular subtypes include luminal A and B tumors, which express estrogen receptor (ER) and progesterone receptor (PR) in various combinations; human epidermal growth factor receptor 2 (HER2)-enriched tumors, which are characterized by the overexpression of HER2; and triple-negative breast cancer (TNBC), which lacks ER/PR/HER2 expression (5). Molecular classification has been shown to be critical for therapeutic guidance and prognosis since HER2-positive and TNBC tumors typically exhibit more aggressive behavior and differential treatment responses (6). Owing to the heterogeneity of TNBC, Lehmann et al. (7) proposed a TNBC sub-classification system comprising six subtypes: basal-like 1/2, mesenchymal/mesenchymal-like, luminal androgen receptor (LAR), and an immunomodulatory group, each displaying unique molecular profiles with variability in prognosis/treatment sensitivity; some show increased chemotherapy responsiveness, whereas others are correlated with increased relapse risk. Another widely used classification, prediction analysis of microarray 50 (PAM50), categorizes breast cancers into luminal A/B, HER2-enriched, basal-like or normal-like subtypes, using a 50-gene transcriptional panel. This framework is clinically relevant because it provides insights into tumor behavior and aids in therapeutic decision-making (8). Although TNBC is frequently considered synonymous with the basal subtype, studies indicate an approximately 80% overlap between these two categories. This high correlation suggests that different classification techniques may lead to distinct interpretations of tumor behavior. However, given their significant molecular and clinical similarities, it is common for findings from TNBC-focused studies to be extrapolated to basal subtypes and *vice versa*. This widely adopted practice arises because researchers often access distinct datasets, some of which are based on immunohistochemical classification (TNBC) and others on transcriptional profiling (basal). Thus, extrapolation serves as a pragmatic tool to broaden the applicability of results despite limitations in standardized classification methods (9).

The TNBC/basal subtype represents the most challenging entity in oncological management and is characterized by complex molecular heterogeneity, the absence of specific therapeutic targets, high aggressiveness, elevated recurrence rates and reduced five-year overall survival (OS). Despite these therapeutic hurdles, recent advances in targeted immunotherapy with poly (ADP-ribose) polymerase (PARP) inhibitors and combination approaches have emerged as promising strategies (10). In this context, bioprospecting through "omics" data analysis has become an important auxiliary strategy, contributing to novel diagnostic/prognostic biomarker identification, mapping underexplored oncogenic pathways and uncovering potential molecular targets, thereby offering innovative perspectives for understanding this tumor subtype (11).

The *ropporin-1* (*ROPN1*) gene was initially identified as a regulator of sperm motility and was first described in human and murine testicular tissues. Current annotations indicate that it encodes a protein predominantly expressed in male reproductive tissues, with functional roles linked to sperm flagellum axoneme formation (12). Subsequent studies revealed *ROPN1* expression in diverse reproductive tissues at relatively low levels (13, 14). In the context of breast cancer, transcriptomic data suggest differential *ROPN1* expression patterns between normal and tumor tissues, with overexpression associated with aggressive malignancies, particularly TNBC subtypes. While the exact mechanistic contribution of *ROPN1* to tumorigenesis remains incompletely understood, its established roles in cellular motility pathways may facilitate invasive/metastatic processes (13).

Materials and Methods

Identification of *ROPN1*

GSE76275 was interrogated via GEO2R (15, 16) to identify DEGs between TNBC and non-TNBC using Benjamini-Hochberg-adjusted $p<0.05$ and $|\log_2 FC| \geq 1.5$. *ROPN1*, among the most dysregulated, was selected for focused TNBC expression and functional analyses.

The Cancer Genome Atlas (TCGA) Data Analysis

TCGA Firehose Legacy data (n = 1108) were retrieved via cBioPortal, excluding 12 male patients, five without age and four without *ROPN1* expression data, yielding 1087 female cases. *ROPN1* levels were merged with clinicopathological data and PAM50 calls from Xena by barcode (17). Cases were dichotomized at the median into low (≤median) and high (>median) groups. Categorical associations used χ^2; continuous data were log-transformed to z-scores (RNA-Seq V2 RSEM), tested for normality (Shapiro-Wilk) and analyzed by Student's t/ANOVA or Mann-Whitney/Kruskal-Wallis. HM450 β-values at the *ROPN1* locus were compared across PAM50 subtypes and correlated with expression via Spearman's test.

Study Methodology: Sweden Cancerome Analysis Network-Breast (SCAN-B) Analysis

RNA-seq from SCAN-B [GSE96058; n=3,678; n=3,273 tumors after excluding replicates/NAs; median follow-up 52 months (18)] were processed in R (gtsummary) (19). *ROPN1* expression was again dichotomized at the median; Wilcoxon rank-sum and χ^2 tests assessed clinicopathological associations. Optimal cut-offs were derived via survminer residual-minimization (20) to generate Kaplan-Meier curves and Cox models (survival package; $p<0.05$), with analyses stratified by basal subtype and chemotherapy status.

GEO Database Analysis

Five GEO datasets (GSE76275, GSE21653, GSE32646, GSE18864, GSE43358) were retrieved and analyzed via GEO2R to compare *ROPN1* probe-specific expression (224191_x_at, 231535_x_at, 233203_at) between groups. Post-analysis outputs were exported and plotted in GraphPad Prism 9 boxplots with consistent scaling and outlier thresholds to visualize cohort-wise expression differences.

Functional Enrichment Analysis and Protein-Protein Interaction Network

To elucidate *ROPN1's* molecular interactions, we performed comprehensive correlation analyses via cBioPortal followed by gene selection for subsequent protein-protein interaction (PPI) network modeling, using STRING-db (https://www.string-db.org/). The selected genes were subjected to rigorous PPI network construction and

pathway enrichment analysis with a stringent interaction confidence threshold (≥0.4) to ensure biological relevance (21). Using STRING-db, potential PPI interaction networks were mapped followed by visualization and computational refinement through Cytoscape 3.10.1 (www.cytoscape.org/).

MethSurv

MethSurv is an R Shiny web portal that uses TCGA CpG beta values (0–1) to perform univariate and multivariate survival analyses with built-in visualization and clustering, with no coding or extra software required (22). In the present study, MethSurv was used to assess survival outcomes using the invasive breast cancer dataset from TCGA, incorporating *ROPN1* as a focal point of our analyses.

Cell Line Culture and Treatment

MCF10A (ATCC CRL-10317) cells were maintained in 1:1 DMEM/F12 supplemented with 5% horse serum, 0.5 µg/mL hydrocortisone, 10 µg/mL insulin, 20 ng/mL EGF and 100 ng/mL cholera toxin. Hs578T (ATCC HTB-126), MDA-MB-231 (ATCC HTB-26), SK-BR-3 (ATCC HTB-30), HCC70 (ATCC CRL-2315), MCF7 (ATCC HTB-22), BT-474 (ATCC HTB-20) and BT-549 (ATCC HTB-122) were cultured in DMEM or RPMI 1640 with 10% FBS and 1% penicillin-streptomycin. All lines were incubated at 37 °C, 5% CO_2, with medium renewed every 48 h until 50–60% confluence. Mycoplasma testing was performed before and after experiments; subcultures used 0.25% trypsin-EDTA.

Concentrations of 5-aza-2′-deoxycytidine (5-aza) and trichostatin A (TSA) were set by Alamar Blue assays to avoid morphological or growth alterations. Cisplatin, doxorubicin and paclitaxel were applied at ½ IC_{50} [CancerRxGene (23)]; SK-BR-3 dosing was performed as described by Hai et al. A single 6 Gy fraction was delivered via an RS2000 irradiator with Gafchromic dosimetry, followed by 48 h recovery and RNA isolation (SV Total RNA, Promega).

cDNA was synthesized from 2 µg RNA (High-Capacity Kit, Thermo Fisher) and quantitative polymerase chain reaction (qPCR) performed (SYBR Green, Applied Biosystems 7500) using primers for *ROPN1* (NM_001394219.1; F: 5′-CCAAAGCCGCCATTAGGGT-3′, R: 5′-GGCTGCCCACTGGATGAG-3′) and GAPDH (NR_152150.2; F: 5′-GACTGTGGTCATGAGTCCTCCC-3′, R: 5′-CAAGATCATCAGCAATGCCTCC-3′). Relative expression was normalized to GAPDH and calculated by $\Delta\Delta C_t$ in triplicate.

Statistical Analysis

Statistical analysis was performed using specialized software. This included SPSS, version 25.0 (IBM Inc., Armonk, NY, USA) and GraphPad, version 7 (California, USA). Data normality was assessed by Shapiro-Wilk test. Categorical variables were compared using χ^2 test; continuous variables employed Student's t-test or ANOVA for normally distributed data and Mann-Whitney or Kruskal-Wallis tests otherwise. Associations were evaluated by Spearman's (non-parametric) rank correlation. Survival outcomes were estimated via Kaplan-Meier curves with log-rank testing and multivariate hazard ratios (HRs) calculated by Cox proportional hazards regression. All tests were two-tailed with significance defined as $p<0.05$.

Results

Differences Observed in TCGA Data

It was observed that high *ROPN1* expression was significantly associated with key clinical and pathological characteristics. Patients in the high *ROPN1* subgroup were more frequently premenopausal ($p = 0.0027$) and exhibited a predominance of hormone receptor-negative tumors (ER-/PR-, $p<0.0001$) and HER2-negative status ($p<0.0001$). Furthermore, high *ROPN1* expression levels were strongly correlated with basal-like and normal-like subtypes based on the PAM50 classification ($p<0.0001$). Among patients with TNBC, the majority exhibited high *ROPN1* expression ($p<0.0001$). Differences in histological type were significant ($p = 0.0013$), whereas TNM staging did not show significant variation between groups ($p = 0.2276$) (Table 1).

Table 1. Clinicopathological characteristics of patients with breast cancer derived from the TCGA database and their associations with *ROPN1* expression levels

Variables	Low		High		*p*
	n		*n*		
Age					
≤50	132	24.30	201	37.00	<0.0001
>50	412	75.70	342	63.00	
Menopause status					
Pre	101	20.60	129	26.70	0.0027
Peri	13	2.60	27	5.60	
Post	377	76.80	327	67.70	
Cancer type detailed					
IDC	418	77.00	383	70.50	0.0013
ILC	80	14.70	126	23.20	
Other	45	8.30	34	6.30	
TNM stage					
Stage 1	80	15.00	100	18.80	0.2276
Stage 2	309	58.10	307	57.80	
Stage 3	131	24.60	117	22.00	
Stage 4	12	2.30	7	1.30	
ER status by IHC					
Negative	44	8.60	194	37.00	<0.0001
Positive	469	91.40	330	63.00	
PR status by IHC					
Negative	113	22.10	228	43.60	<0.0001
Positive	398	77.90	295	56.40	
HER2 status by IHC					
Negative	250	70.00	308	85.10	<0.0001
Positive	107	30.00	54	14.90	
PAM50 classification					
Basal	5	1.10	135	35.20	<0.0001
HER2	45	9.90	22	5.70	
Luminal A	243	53.60	173	45.20	
Luminal B	158	34.90	31	8.10	
Normal-like	2	0.40	22	5.70	

Table 1. Continued

Variables	Low		High		*p*
	n		*n*		
TNBC status					
nTNBC	496	98.2	356	76.9	<0.0001
TNBC	9	1.8	107	23.1	

ER: Estrogen receptor; HER2: Human epidermal growth factor receptor 2; IDC: Invasive ductal carcinoma; IHC: Immunohistochemistry; ILC: Invasive lobular carcinoma; PAM50: Prediction analysis of microarray 50 (50-gene panel used for molecular classification); Peri: Perimenopausal; Post: Postmenopausal; PR: Progesterone receptor; Pre: Premenopausal; TNBC: Triple-negative breast cancer; TNM: Tumor, node, metastasis (staging system for tumor size, lymph node involvement, and metastasis); TCGA: The Cancer Genome Atlas

The pattern of *ROPN1* expression was analyzed in different clinicopathological contexts, as illustrated in the graphs (Figure 1A-F). In each graph, the expression of *ROPN1* was compared among subgroups with distinct clinical characteristics and significant variations emerged. *ROPN1* mRNA expression was higher in ER-negative, PR-negative, and HER2-positive tumors compared with their opposite counterparts (all $p<0.0001$; Figure 1A-1C). Expression varied by menopausal status ($p = 0.0171$; Figure 1D) and was elevated in invasive ductal carcinoma versus other histological types ($p = 0.0126$) (Figure 1E). Basal-like tumors showed the highest *ROPN1* levels among molecular subtypes ($p<0.0001$) (Figure 1F). Inverse correlation between *ROPN1* mRNA levels and promoter methylation was observed in unstratified TCGA breast tumors (Figure 2A; r = –0.41; $p<0.0001$) and was stronger in basal-like tumors (Figure 2B; r = –0.55; $p<0.0001$). Stratification by clinical subtype highlighted significantly lower methylation in basal-like versus HER2-enriched, luminal A/B and normal-like tumors (Figure 2C, D). Survival analysis via MethSurv showed that hypermethylation at cg00101712 and cg09298623 correlated with improved prognosis [Figure 2E; HR = 0.59; 95% confidence interval (CI): 0.38–0.92; $p = 0.016$; Figure 2F; HR = 0.49; 95% CI: 0.31–0.78; $p = 0.0014$].

Global correlation via cBioPortal identified 14,462 *ROPN1*-associated genes; the top 20 positive and 20 negative correlates were input into STRING to generate a PPI network (Figure 2G). Positively linked nodes included *ROPN1B, SOX10, FABP7, SOSTDC1, SFRP1, BCL11A, FOXC1* and *MIA*; negatively linked nodes comprised *BCAS1, GATA3, AR, ARMT1, FOXA1, XBP1, WWP1, ESR1* and *TMBIM6*. STRING enrichment highlighted glandular morphogenesis and hormonal response pathways, prostate gland epithelium and glandular acinus development; branched and epithelial tube morphogenesis; and cellular response to estrogenic stimuli, underscoring the interplay of gland architecture and hormone signaling in breast cancer progression (Figure 2H).

Prognostic Insights from the SCAN-B Study on *ROPN1* Expression in Breast Cancer

SCAN-B RNA-seq data recapitulated TCGA associations: High (n = 1,636) versus low (n = 1,637) *ROPN1* expression groups differed in age ≤55 y (36%; $p<0.001$), tumor size ≤17 cm (56%; $p<0.001$), ER+ (89% *versus* 96% and PR+ 84% *versus* 90%; $p<0.001$), luminal A enrichment in high expression (55%) and luminal B/HER2 in low expression ($p<0.001$), endocrine therapy use in high *ROPN1* expression (71%; $p<0.001$) and chemotherapy in low expression

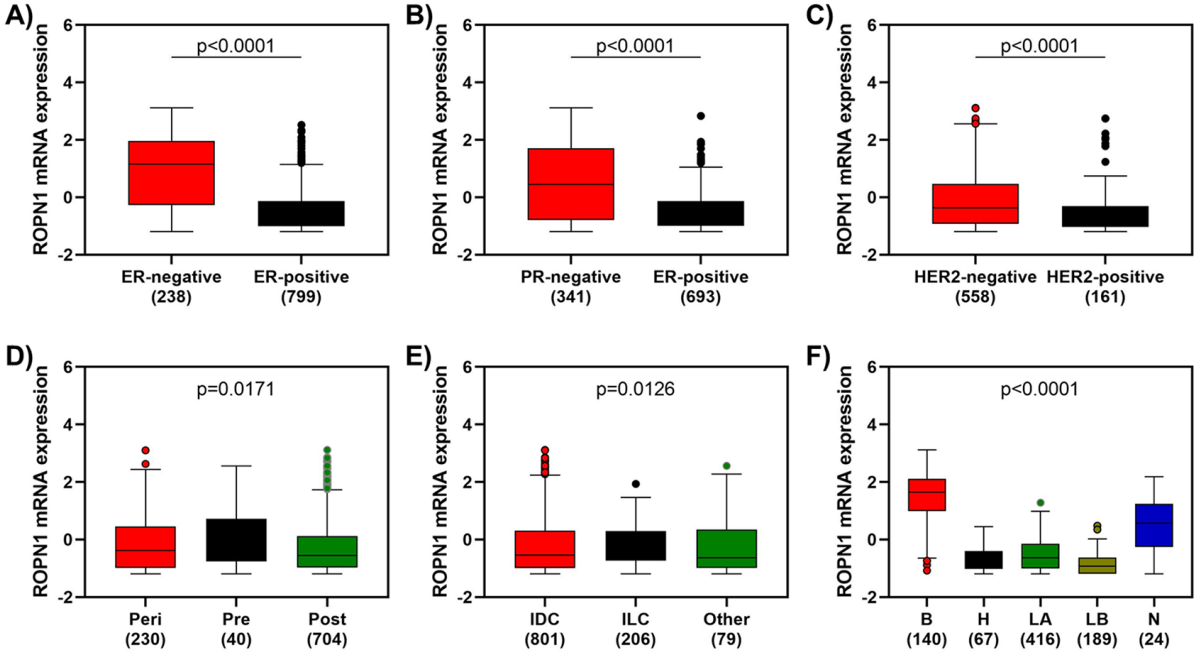

Figure 1. *ROPN1* expression patterns in different clinical-pathological contexts of breast cancer. The graphs show comparisons of *ROPN1* expression among subgroups for (A) estrogen receptor, (B) progesterone receptor, (C) HER2, (D) menopausal status, (E) histological type, and (F) molecular subtypes according to the PAM50 classification. Dunn's multiple comparisons test was applied, and differences between the basal and HER2, luminal A or luminal B subtypes were significant ($p<0.0001$), whereas only the difference between the basal and normal-like subtypes was not significant ($p = 0.2751$)

ER: Estrogen receptor; PR: Progesterone receptor; HER2: Human epidermal growth factor receptor type II; Peri: Perimenopausal; Pre: Premenopausal; Post: Postmenopausal; IDC: Invasive ductal carcinoma; ILC: Invasive lobular carcinoma; B: Basal; H: HER2; LA: Luminal A; LB: Luminal B; N: Normal-like

(62%; p = 0.031) groups; nodal status was comparable (63% negative; p>0.9) (Supplementary Table1).

ROPN1 mRNA was elevated in ER–, PR– and HER2– tumors (all p<0.0001), and in tumors with high Ki-67 staining (p = 0.0191), as well as in tumors in which endocrine therapy was not used (p<0.0001). Expression was highest in basal and HER2-enriched subtypes, decreasing through luminal A and B and normal-like (p<0.0001), indicating an association with aggressive phenotypes (Supplementary Figure 1).

High *ROPN1* expression predicted poorer OS in SCAN-B (Figure 3A; HR = 2.17; 95% CI: 1.61–2.94; p<0.0001), with a pronounced effect in basal tumors (Figure 3B; HR = 1.85; 95% CI: 1.02–3.33; p = 0.041). In chemotherapy-treated patients, high *ROPN1* remained adverse (Figure 3C; HR = 2.86; 95% CI: 1.28–6.25; p = 0.01), and in untreated patients the mortality risk was even higher (Figure 3D; HR = 4.55; 95% CI: 1.33–14.29; p = 0.01).

Probes 224191_x_at (Figure 3E), 231535_x_at (Figure 3F) and 233203_at (Figure 3G) showed consistent *ROPN1* overexpression in TNBC versus non-triple negative subtypes across GSE76275, GSE21653, GSE32646, GSE18864 and GSE43358, underscoring its association with invasive tumor phenotypes.

Transcriptional Modulation of *ROPN1* in Breast Cancer Cell Lines

After culturing non-tumoral mammary tissue cell lines and other representative malignant phenotypes were cultured, total RNA extraction was performed for reverse transcription-qPCR analysis. When MCF10A was used as a reference, SKBR3 and MCF7 cells exhibited *ROPN1* expression levels that were more than 2,000 times greater. The BT474, HS-578T, BT549, and MDA-MB-231 lines expressed increases ranging from 0.5 to approximately 60 times. Notably, among those analyzed, HCC70 demonstrated a *ROPN1*

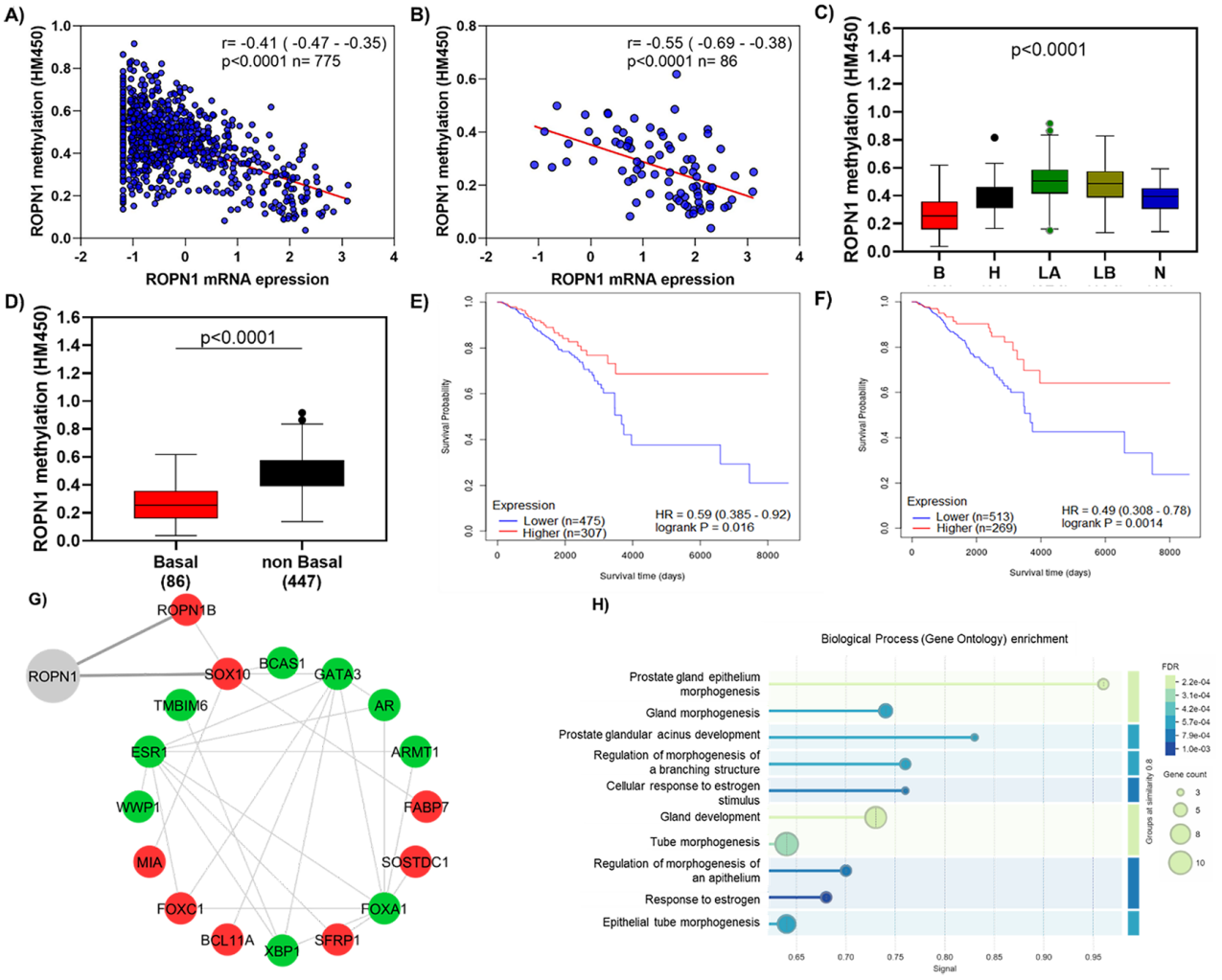

Figure 2. Methylation profile of *ROPN1* in breast cancer patients. (A) Correlation between *ROPN1* mRNA levels and methylation in a population of breast cancer patients. (B) Specific correlation for the basal subtype of breast cancer, where the negative correlation is more pronounced. (C) Methylation pattern of *ROPN1* according to the PAM50 classification. (D) Comparison of *ROPN1* methylation in the clinical profiles of basal and non-basal breast cancer patients. (E) OS analysis based on the methylation pattern of the *ROPN1* body opening site cg00101712. (F) OS analysis based on the methylation profile of *ROPN1* in TSS1500 N-shore cg09298623. (G) The PPI network was constructed using the STRING database, employing the top 40 genes correlated with *ROPN1* from the TCGA Firehose Legacy database. Red represents genes positively correlated with *ROPN1*, whereas green indicates genes negatively correlated with *ROPN1*. (H) Pathway enrichment analysis

B: Basal; H: HER2; LA: Luminal A; LB: Luminal B; N: Normal-like; PPI: Protein-protein interaction; PAM50: Prediction analysis of microarray 50; HER2: Human epidermal growth factor receptor 2

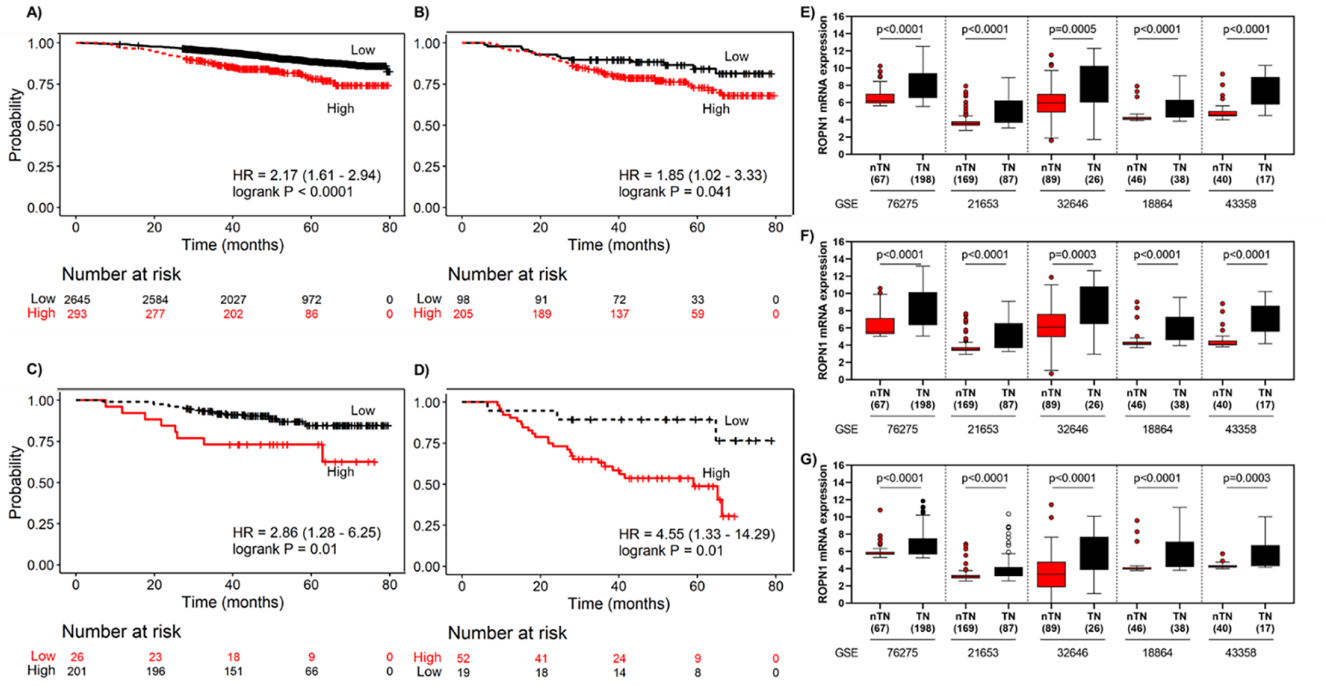

Figure 3. Associations between *ROPN1* expression and survival in breast cancer patients. (A) Overall survival analysis of all breast cancer patients. (B) Stratified survival of patients with the basal subtype of breast cancer. (C) Impact of *ROPN1* expression on the survival of basal breast cancer patients undergoing chemotherapy. (D) Comparative survival analysis of basal breast cancer patients who did not receive chemotherapy. Data were obtained from the GSE96058 study and analyzed via Kaplan-Meier curves. The "Low" and "High" categories refer to patient classification based on *ROPN1* gene expression levels, with "Low" indicating expression below the established cut-off value, and "High" indicating expression above this threshold. Expression pattern of *ROPN1* in different cohorts. The probes 224191_x_at (E), 231535_x_at (F), and 233203_at (G) were evaluated using datasets available in the GEO database, identified as GSE76275, GSE21653, GSE32646, GSE18864, and GSE43358, respectively

expression level over 7,000 times greater than that of MCF10A, highlighting the increased expression of this gene in certain tumor contexts (Figure 4A).

The cell lines were subsequently treated with chemotherapeutics and radiotherapy to evaluate any transcriptional modifications. MCF7 cells presented a greater fold change than did wild-type cells (untreated), with increases of 23%, 3%, and 26% after exposure to cisplatin, doxorubicin, and paclitaxel, respectively. In contrast, irradiation with 6 Grays resulted in a drastic decrease in *ROPN1* (Figure 4B). For the SKBR3 line, there was a decrease of approximately 40% after both cisplatin and paclitaxel treatment, although doxorubicin and radiation did not reduce *ROPN1* expression levels in this cell line (Figure 4C). In BT474 cells, cisplatin and doxorubicin induced decreases of 48% and 38%, respectively. Conversely, irradiation led to a 25% increase in the transcript level (Figure 4D). For the HCC70 line, which, among the lines used, was the one that expressed *ROPN1* at the highest level, all the treatments induced a decrease in the level of this transcript, which was most evident with cisplatin, with which a 63% reduction was achieved (Figure 4E). Similarly, HS578T cells also exhibited a reduction of approximately 50% in response to cisplatin, doxorubicin, and irradiation and a 30% decrease after paclitaxel treatment (Figure 4F). BT549 cell expression of *ROPN1* was were reduced by 21% only after cisplatin treatment and significantly increased by 197% and 293% after doxorubicin and paclitaxel treatment, respectively (Figure 4G). Finally, for MDA-MB231 cells, in which the expression levels were close to those found in the MCF10A reference cells, all the treatments induced a significant increase in *ROPN1* (Figure 4H). The HS578T line was also treated with 5-aza and TSA, which resulted in increases in the expression of *ROPN1* by 9.5-fold and 4.9-fold, respectively (Figure 4I).

Discussion and Conclusion

Breast cancer remains a leading cause of female cancer mortality, with TNBC/basal tumors exhibiting high recurrence and chemoresistance. Biomarker discovery is therefore essential for enhanced risk stratification and therapeutic decision-making. *ROPN1* emerged as a candidate, showing elevated expression in TNBC/basal cases and consistent association with poor survival. Our data indicate that high *ROPN1* expression is consistently associated with poor OS in breast cancer patients, especially those with basal-like subtype, which is known for its high degree of aggressiveness and poor prognosis. Risk analysis showed that patients with high *ROPN1* expression who were not treated with chemotherapy had an HR of 4.55 (Figure 3D), indicating a robust association between *ROPN1* expression and unfavorable outcomes. Among patients who received chemotherapy, high levels of *ROPN1* also correlated with poorer prognosis (HR = 2.53). These findings position *ROPN1* as a potent prognostic marker of aggressive breast cancer and a potential predictor of limited chemotherapy response, underscoring the need for personalized treatment strategies.

Previous findings by Liu et al. (13) showed that *ROPN1* is overexpressed in TNBC, enhancing migration, invasion and metastasis via RhoA activation. Overexpression increased actin stress fibers and contractility, while *ROPN1* silencing reduced invasiveness

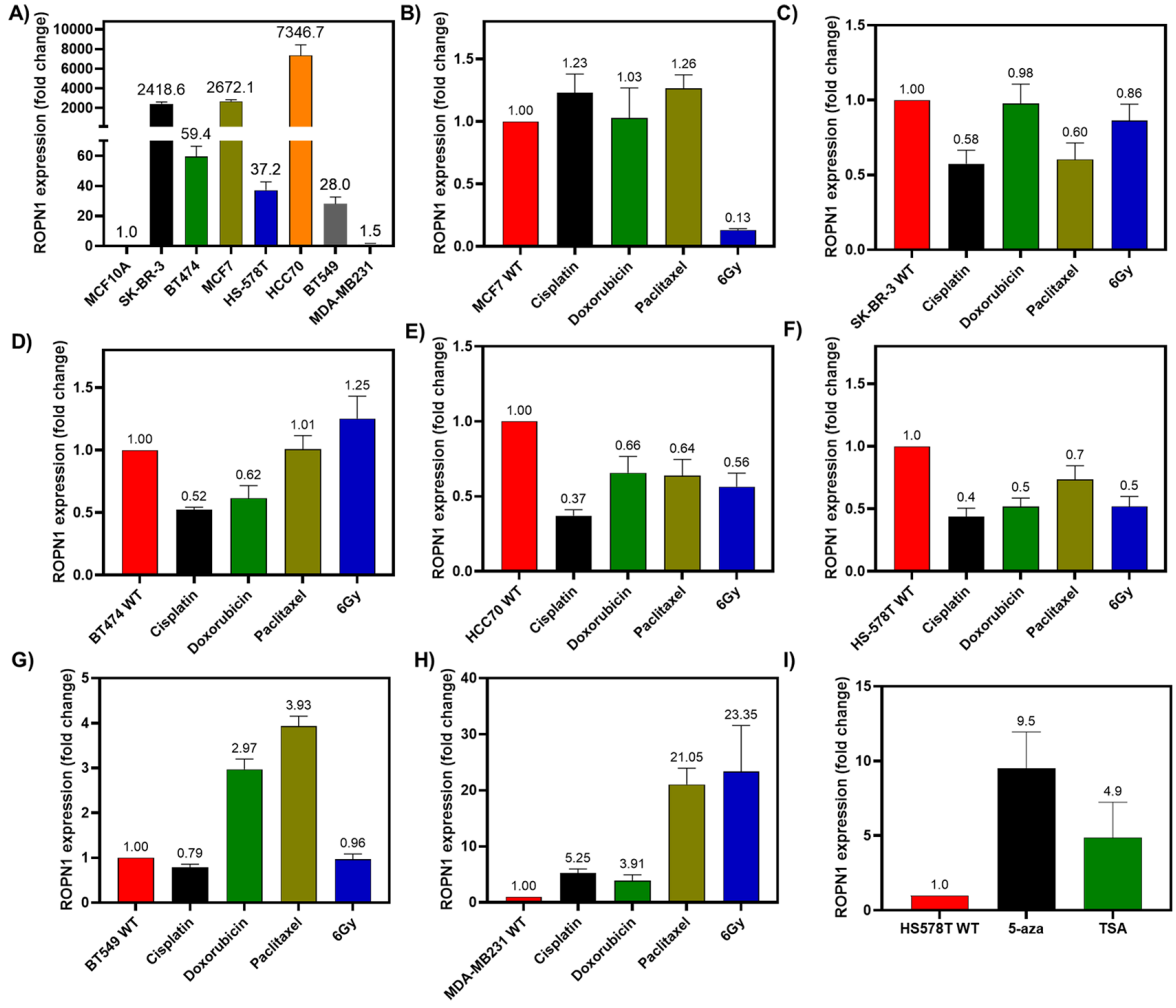

Figure 4. Expression of *ROPN1* in breast cancer cell lines and the effects of different treatments. (A) Basal transcription levels of *ROPN1* in a panel of mammary cell lines, including distinct tumor subtypes. (B-H) Variation in *ROPN1* expression after treatment with cisplatin, doxorubicin, paclitaxel, or radiotherapy. (I) Modulation of *ROPN1* expression in response to the epigenetic-acting drugs 5-Aza and trichostatin A

and metastasis *in vitro* and *in vivo*. Kortleve et al. (24) validated *ROPN1* as a prognostic and therapeutic target in TNBC, showing strong expression in >90% of primary and metastatic tumors, with minimal expression in normal tissues, except testis. In patient-derived and murine models, anti-*ROPN1* TCR-T cells effectively eliminated *ROPN1*+ tumors, outperforming cisplatin and sacituzumab govitecan. *ROPN1* expression correlated with metastasis and poor prognosis. These findings align with our results, supporting the translational value of *ROPN1* as a biomarker and therapeutic target in TNBC.

In our PPI analysis, *ROPN1B* and *SOX10* emerged as key genes positively correlated with *ROPN1*. *ROPN1B*, a cytoskeleton-related protein sharing 96% sequence homology with *ROPN1*, may act synergistically to promote invasiveness. Da Gama Duarte et al. (25) reported a strong correlation between *ROPN1* and *ROPN1B* in melanoma ($r = 0.86$, $p = 8.71\times10^{-4}$), associating both with motility, chemoresistance and immune modulation. *SOX10*, which also correlated with *ROPN1*, drives mesenchymal traits and drug resistance in TNBC (26-28), suggesting that their co-expression may enhance tumor plasticity and therapeutic evasion.

The network also included clinically relevant genes, such as *ESR1*, *AR* and *FOXA1*, all downregulated or absent in TNBC/basal tumors. *ESR1*, a key marker in luminal subtypes, serves as both a prognostic indicator and therapeutic target. *AR*, though expressed in a subset of TNBCs, lacks the favorable impact seen with *ESR1* but may serve as a target in LAR tumors (10). *FOXA1*, a transcriptional cofactor for both *ESR1* and *AR*, promotes epithelial identity in luminal cancers but is minimally expressed in TNBC, supporting its undifferentiated and aggressive profile (29, 30).

Chemotherapeutic treatments and radiotherapy have heterogeneous effects on *ROPN1* levels, depending on the cell line and the therapeutic agent used. Among the parental lines analyzed, HCC70 exhibited an increase in *ROPN1* expression of more than 7,000 times, highlighting the unique behavior of the TNBC subtype, which is highly aggressive and has a poor prognosis (7). This overexpression may be associated with the role of *ROPN1* in fundamental biological processes, such as cell motility, which directly contributes to tumor migration and invasion. Indeed, previous studies have demonstrated that *ROPN1* plays an active role in tumor progression, especially in TNBC. Wu and collaborators reported that the overexpression of *ROPN1* was associated with a significant increase in cell migration and invasion, which is mediated by the activation of RhoA, a GTPase essential for cytoskeletal organization (24). This activation leads to actin reorganization, promoting the formation of cellular protrusions and

facilitating tumor spread. Furthermore, *in vivo* models have shown that *ROPN1* not only enhances metastasis but also that its suppression significantly reduces tumor dissemination (24).

By analyzing the effects of chemotherapeutic agents on a selection of cell lines, we propose a relevant translational hypothesis. We observed that, under certain conditions, treatments did not reduce or even increased the levels of *ROPN1*, as noted in BT549 cells after exposure to doxorubicin and paclitaxel. Considering the findings of Wu et al. on the prometastatic role of *ROPN1*, these results suggest that the persistence or elevation of this transcript following chemotherapy may represent an adaptive mechanism of tumor cells, promoting therapeutic resistance and enhancing their migratory and survival capabilities. This hypothesis becomes even more pertinent when the clinical survival data of patients treated with chemotherapy are reviewed (Figure 3C), where high expression of *ROPN1* was associated with a poorer prognosis, even after treatment.

The observed relationship between *ROPN1* expression and its methylation in breast cancer suggests that epigenetic mechanisms may be involved in the regulation of this gene, particularly in the context of more aggressive subtypes, such as HER2-positive breast cancer and TNBC/basal cancer. This pattern of hypomethylation associated with *ROPN1* overexpression indicates that DNA methylation might act as a modulator of gene expression in highly proliferative cancers with increased invasive capacity. To date, only the study by Atanackovic and colleagues has evaluated possible associated epigenetic mechanisms through pharmacological treatment in cell lines derived from acute myeloid leukemia (AML) (31). In their study, treatment with TSA and decitabine or their combination did not result in positive modulation of *ROPN1*, which is poorly expressed in AML, suggesting that other regulatory mechanisms may occur in these lines, such as post-transcriptional regulation mediated by microRNAs or interactions with inhibitory transcription factors. Of note, our *in vitro* experiments revealed a significant increase in *ROPN1* expression after treatment with 5-aza or TSA, with elevated levels of 9.5- and 4.9-fold, respectively. These results reinforce our *in silico* findings and suggest a distinct epigenetic role of *ROPN1* in breast cancer, especially considering the contrast with the AML model. These data highlight the importance of investigating how the epigenetic deregulation of *ROPN1* influences tumor behavior in different biological contexts, especially in more aggressive breast subtypes, and exploring whether hypomethylation and overexpression of this gene have direct functional impacts on tumor progression and therapeutic response. Moreover, we observed that low methylation in the regions cg09298623 and cg00101712 was associated with worse OS in patients with this phenomenon. The increased expression of *ROPN1*, which is mediated by a reduction in methylation, may represent a phenotypic adaptation of the tumor that facilitates cell invasion and metastasis, which can lead to a worsened clinical outcome for these patients.

Further studies are needed to clarify how epigenetic changes drive tumor aggressiveness and to define the functional role of *ROPN1* in breast cancer progression and therapy response. While our multicohort analysis offers strong associative evidence, functional validation (e.g., CRISPR/Cas9) is required to confirm causality in chemoresistance. Prospective cohorts and mechanistic studies will be key to validating *ROPN1* expression as a predictive biomarker, potentially guiding patient stratification and improving therapeutic outcomes in high-risk cases.

Study Limitations

This study has limitations, including the absence of validation in patient-derived tumor samples and reliance on public gene expression datasets. In addition, the interactions between *ROPN1*, tumor subtypes, and therapeutic contexts, especially drug combinations, remain incompletely characterized. Further studies are needed to validate these findings and clarify the role of *ROPN1* in breast cancer biology.

ROPN1 is markedly overexpressed in hormone receptor–negative and triple-negative/basal-like breast cancers, where it predicts significantly poorer OS. Its prognostic value persists regardless of chemotherapy status, high *ROPN1* expression doubles mortality risk in treated patients and quadruples it when treatment is absent, underscoring its utility for risk stratification. An inverse relationship between DNA methylation and *ROPN1* expression further links hypomethylation to adverse outcomes. *In vitro*, *ROPN1* expression following chemotherapeutics and radiotherapy was variable in different cell lines, with some agents inducing upregulation suggesting adaptive resistance mechanisms. Collectively, these findings position *ROPN1* and its protein product as both a robust prognostic and predictive biomarker and a candidate therapeutic target for high-risk breast cancer subgroups.

Acknowledgements

We sincerely thank Prof. Dr. Luisa Villa for graciously providing access to her laboratory facilities, which made the execution of this study possible. We express our sincere gratitude to Prof. Dr. Sandra Gonzalez and Prof. MSc. Nancy Ramona Segovia Coronel for their invaluable support to scientific research.

Ethics

Ethics Committee Approval: Not necessary.

Informed Consent: Not necessary.

Footnotes

Authorship Contributions

Concept: R.C.C., D.R.d.B.; Design: R.C.C., D.R.d.B.; Data Collection or Processing: R.C.C., A.G.C., D.R.d.B.; Analysis or Interpretation: R.C.C., D.R.d.B.; Literature Search: R.C.C., O.M.G., C.J.M., D.R.d.B.; Writing: R.C.C., A.G.C., O.M.G., C.J.M., D.R.d.B

Conflict of Interest: No conflict of interest was declared by the authors.

Financial Disclosure: The authors declared that this study received no financial support.

References

1. Sung H, Ferlay J, Siegel RL, Laversanne M, Soerjomataram I, Jemal A, et al. Global Cancer Statistics 2020: GLOBOCAN estimates of incidence and mortality worldwide for 36 cancers in 185 countries. CA Cancer J Clin. 2021; 71: 209-249. (PMID: 33538338) [Crossref]
2. DeSantis CE, Ma J, Gaudet MM, Newman LA, Miller KD, Goding Sauer A, et al. Breast cancer statistics, 2019. CA Cancer J Clin. 2019; 69: 438-451. (PMID: 31577379) [Crossref]
3. Torre LA, Siegel RL, Ward EM, Jemal A. Global cancer incidence and mortality rates and trends--an update. Cancer Epidemiol Biomarkers Prev. 2016; 25: 16-27. (PMID: 26667886) [Crossref]

4. Arnold M, Morgan E, Rumgay H, Mafra A, Singh D, Laversanne M, et al. Current and future burden of breast cancer: global statistics for 2020 and 2040. Breast. 2022; 66: 15-23. (PMID: 36084384) [Crossref]
5. Popa M-T, Noditi A, Peleaşa T-M, Stoleru S, Blidaru A. Breast cancer: a heterogeneous pathology. prognostic and predictive factors - a narrative review. Chirurgia (Bucur). 2025; 120: 32. [Crossref]
6. Zhang X. Molecular classification of breast cancer: relevance and challenges. Arch Pathol Lab Med. 2023; 147: 46-51. (PMID: 36136295) [Crossref]
7. Lehmann BD, Bauer JA, Chen X, Sanders ME, Chakravarthy AB, Shyr Y, et al. Identification of human triple-negative breast cancer subtypes and preclinical models for selection of targeted therapies. J Clin Invest. 2011; 121: 2750-2767. (PMID: 21633166) [Crossref]
8. Kensler KH, Sankar VN, Wang J, Zhang X, Rubadue CA, Baker GM, et al. PAM50 molecular intrinsic subtypes in the Nurses' Health Study Cohorts. Cancer Epidemiol Biomarkers Prev. 2019; 28: 798-806. (PMID: 30591591) [Crossref]
9. Zagami P, Carey LA. Triple negative breast cancer: pitfalls and progress. NPJ Breast Cancer. 2022; 8: 95. (PMID: 35987766) [Crossref]
10. Xiong N, Wu H, Yu Z. Advancements and challenges in triple-negative breast cancer: a comprehensive review of therapeutic and diagnostic strategies. Front Oncol. 2024; 14: 1405491. (PMID: 38863622) [Crossref]
11. Jiang P, Sinha S, Aldape K, Hannenhalli S, Sahinalp C, Ruppin E. Big data in basic and translational cancer research. Nat Rev Cancer. 2022; 22: 625-639. (PMID: 36064595) [Crossref]
12. Gao S, Chen Z, Shi J, Chen Z, Yun D, Li X, et al. Sperm immotility is associated with epididymis metabolism disorder in mice under obstructive azoospermia. FASEB J. 2023; 37: e23081. (PMID: 37410071) [Crossref]
13. Liu Q, Huang X, Li Q, He L, Li S, Chen X, et al. Rhophilin-associated tail protein 1 promotes migration and metastasis in triple negative breast cancer via activation of RhoA. FASEB J. 2020; 34: 9959-9971. (PMID: 32427399) [Crossref]
14. Adeola HA, Smith M, Kaestner L, Blackburn JM, Zerbini LF. Novel potential serological prostate cancer biomarkers using CT100+ cancer antigen microarray platform in a multi-cultural South African cohort. Oncotarget. 2016; 7: 13945-13964. (PMID: 26885621) [Crossref]
15. de Bastos DR, Conceição MPF, Michelli APP, Leite JMRS, da Silva RA, Cintra RC, et al. An *in silico* analysis identified FZD9 as a potential prognostic biomarker in triple-negative breast cancer patients. Eur J Breast Health. 2020; 17: 42-52. (PMID: 33796830) [Crossref]
16. Céspedes AG, Conceição MPF, de Bastos DR, de Grazia GÁ, Leite JMRS, do Nascimento RG, et al. Altered expression of CYSLTR1 is associated with adverse clinical outcome in triple negative breast tumors: an *in silico* approach. Eur J Breast Health. 2023; 19: 148-158. (PMID: 37025579) [Crossref]
17. Goldman MJ, Craft B, Hastie M, Repečka K, McDade F, Kamath A, et al. Visualizing and interpreting cancer genomics data via the Xena platform. Nat Biotechnol. 2020; 38: 675-678. (PMID: 32444850) [Crossref]
18. Brueffer C, Vallon-Christersson J, Grabau D, Ehinger A, Häkkinen J, Hegardt C, et al. Clinical value of RNA sequencing-based classifiers for prediction of the five conventional breast cancer biomarkers: a report from the population-based multicenter sweden cancerome analysis network-breast initiative. JCO Precis Oncol. 2018; 2: PO.17.00135. (PMID: 32913985) [Crossref]
19. Sjoberg DD, Whiting K, Curry M, Lavery JA, Larmarange J. Reproducible summary tables with the gtsummary package. R J. 2021; 13: 570. [Crossref]
20. Kassambara A. Survminer: drawing survival curves using "ggplot2." 2023. Accessed in December 2024. [Crossref]
21. Szklarczyk D, Kirsch R, Koutrouli M, Nastou K, Mehryary F, Hachilif R, et al. The STRING database in 2023: protein-protein association networks and functional enrichment analyses for any sequenced genome of interest. Nucleic Acids Res. 2023; 51: D638-D646. (PMID: 36370105) [Crossref]
22. Modhukur V, Iljasenko T, Metsalu T, Lokk K, Laisk-Podar T, Vilo J. MethSurv: a web tool to perform multivariable survival analysis using DNA methylation data. Epigenomics. 2018; 10: 277-288. (PMID: 29264942) [Crossref]
23. Cokelaer T, Chen E, Iorio F, Menden MP, Lightfoot H, Saez-Rodriguez J, et al. GDSCTools for mining pharmacogenomic interactions in cancer. Bioinformatics. 2018; 34: 1226-1228. (PMID: 29186349) [Crossref]
24. Kortleve D, Hammerl D, van Brakel M, Wijers R, Roelofs D, Kroese K, et al. TCR-engineered T cells directed against ropporin-1 constitute a safe and effective treatment for triple-negative breast cancer. Cancer Discov. 2024; 14: 2450-2470. (PMID: 39172012) [Crossref]
25. Da Gama Duarte J, Woods K, Quigley LT, Deceneux C, Tutuka C, Witkowski T, et al. Ropporin-1 and 1B are widely expressed in human melanoma and evoke strong humoral immune responses. Cancers (Basel). 2021; 13: 1805. (PMID: 33918976) [Crossref]
26. Man K-H, Wu Y, Gao Z, Spreng A-S, Keding J, Mangei J, et al. SOX10 mediates glioblastoma cell-state plasticity. EMBO Rep. 2024 ;25: 5113-5140. [Crossref]
27. Yang K, Yun F, Shi L, Liu X, Jia YF. SOX10 promotes the malignant biological behavior of basal-like breast cancer cells by regulating EMT process. Heliyon. 2023; 9: e23162. [Crossref]
28. Feng W, Liu S, Zhu R, Li B, Zhu Z, Yang J, et al. SOX10 induced Nestin expression regulates cancer stem cell properties of TNBC cells. Biochem Biophys Res Commun. 2017; 485: 522-528. (PMID: 28189679) [Crossref]
29. Glont SE, Chernukhin I, Carroll JS. Comprehensive genomic analysis reveals that the pioneering function of FOXA1 is independent of hormonal signaling. Cell Rep. 2019; 26: 2558-2565.e3. (PMID: 30840881) [Crossref]
30. Dai X, Cheng H, Chen X, Li T, Zhang J, Jin G, et al. FOXA1 is prognostic of triple negative breast cancers by transcriptionally suppressing *SOD2* and *IL6*. Int J Biol Sci. 2019; 15: 1030-1041. (PMID: 31182923) [Crossref]
31. Atanackovic D, Luetkens T, Kloth B, Fuchs G, Cao Y, Hildebrandt Y, et al. Cancer-testis antigen expression and its epigenetic modulation in acute myeloid leukemia. Am J Hematol. 2011; 86: 918-922. (PMID: 21898529) [Crossref]

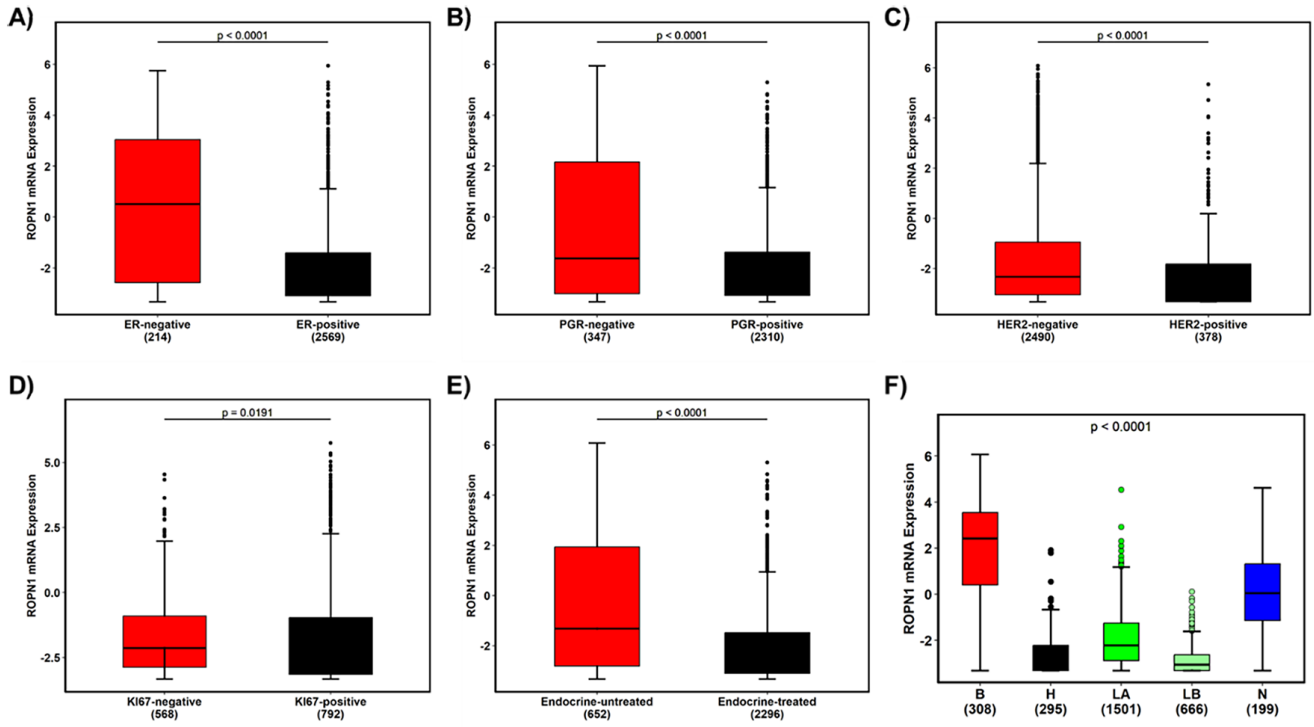

Supplementary Figure 1. Expression pattern of *ROPN1* in patients with breast cancer from the Sweden Cancerome Analysis Network-Breast (SCAN-B) study. Transcriptional levels of *ROPN1* based on (A) estrogen receptor, (B) progesterone receptor, (C) human epidermal growth factor receptor 2, (D) the proliferation marker Ki-67, (E) endocrine treatment, and (F) Prediction analysis of microarray 50 classification

Supplementary Table 1. Clinicopathological characteristics of patients with breast cancer derived from the Sweden Cancerome Analysis Network-Breast study and their associations with *ROPN1* expression

Variables	High		Low		p
	n = 1.636	%	*n* = 1.637	%	
Age					<0.001
≤55	527	36	372	25	
>55	955	64	1.115	75	
Tumor size group					<0.001
≤17 cm	813	56	705	48	
>17 cm	651	44	768	52	
Lymph node status					>0.9
Negative	906	63	910	63	
Positive	533	37	531	37	
ER status					<0.001
No	152	11	62	4	
Yes	1.198	89	1.371	96	
PR status					<0.001
No	205	16	142	10	
Yes	1.091	84	1.219	90	
HER2 status					0.009
No	1.261	88	1.229	85	
Yes	164	12	214	15	
Ki-67 status					0.001
No	318	46	250	37	
Yes	372	54	420	63	
NHG					<0.001
G1	259	18	190	13	
G2	680	47	711	48	
G3	505	35	565	39	
PAM50 subtype					<0.001
Basal	279	19	29	2	
HER2	91	6	204	14	
Luminal A	821	55	680	46	
Luminal B	103	7	563	38	
Normal-like	188	13	11	0.7	
Chemo treated					0.031
No	848	58	911	62	
Yes	622	42	568	38	
Endocrine treated					<0.001
No	424	29	228	15	
Yes	1.045	71	1.251	85	

Pearson's chi-squared test; ER: Estrogen receptor; PR: Progesterone receptor; HER2: Human epidermal growth factor receptor 2; PAM50: Prediction analysis of microarray 50 (50-gene panel used for molecular classification); NHG: Nottingham histologic grade